



Cite this: *Polym. Chem.*, 2015, 6, 3942

PNIPAM-based heteroarm star-graft quarterpolymers: synthesis, characterization and pH-dependent thermoresponsiveness in aqueous media†

Zacharoula Iatridi,^a M. M. Soledad Lencina^a and Constantinos Tsitsilianis*^{a,b}

Heteroarm star-graft quarterpolymers $PS_n[P2VP-b-(PAA-g-PNIPAM)]_n$ bearing two different kinds of arms: a short polystyrene (PS) and a longer poly(2-vinyl pyridine)-*b*-poly(acrylic acid) (P2VP-*b*-PAA) block copolymer arm, grafted by PNIPAM chains onto the outer PAA segments, were synthesized by a three-pot multi-step reaction procedure. Thanks to the pH dependent ionization of P2VP and PAA blocks, as well as the thermo-sensitivity of the PNIPAM grafting chains, these star-graft quarterpolymers exhibited multi-functional responsive behavior in aqueous media. Upon heating the aqueous star-graft solutions, intermolecular hydrophobic association was observed above a critical temperature, defined as T_{ASS} , which was affected by the electrostatic interactions exerted by the weak polyelectrolyte P2VP and PAA segments. This effect led to the appearance of a gel phase at concentrated solutions ($C_p = 3$ wt%). All the observed phenomena depend strongly on the solution conditions and the macromolecular characteristics, namely pH and ionic strength along with the number of arms and the PNIPAM grafting density. The promising preliminary results of this study show that aqueous formulations of these star-graft macromolecules, either in low or high polymer concentrations, could find potential applications as "smart" multi-compartmentalized nanocarriers and/or hydrogels.

Received 18th March 2015,
Accepted 9th April 2015

DOI: 10.1039/c5py00393h

www.rsc.org/polymers

1. Introduction

Star-shaped copolymers constitute a unique type of macromolecules that has received increasing attention over the past years, due to their special architecture, topological symmetry, controllable monomer density, high chain-end functionality and interesting properties that can be tuned by varying the macromolecular features, *i.e.* number, topology and functionality of the arms.^{1–3} Due to their fascinating properties, star copolymers can serve as unimolecular containers for drug delivery^{4–7} and as catalysts^{8–11} or dispersants¹² or can be used for the synthesis of inorganic particles,^{13–16} in emulsion preparation^{17–19} and complexation with biomolecules for gene delivery.^{20,21} A variety of star copolymers exhibiting specific

block/arm topologies like miktoarm stars,^{22–27} star block copolymers,^{28,29} random-block star terpolymers,³⁰ symmetric and asymmetric heteroarm star block copolymers^{31–33} have been prepared by "living" controlled polymerization methods.^{34–45} Numerous studies have been focused on the self-assembly of star-shaped block copolymers and terpolymers in aqueous controlling environments.² An important class of star polymers are the stimuli responsive stars that are polymers bearing block/arms undergoing sharp phase transitions upon responding to external stimuli like pH,^{25,32,46–54} temperature,^{24,27,29,55–57} ionic strength or combinations of them.^{58–61}

In previous articles we have reported the synthesis and characterization of multisegmented heteroarm star block terpolymers, comprising n polystyrene and n poly(2-vinylpyridine)-*b*-poly(acrylic acid) diblock copolymer arms all emanating from a tightly crosslinked poly(divinylbenzene) (PDVB) common nodule $[PS_n(P2VP-b-PAA)_n]$ along with their self-assembly behavior in aqueous solutions and at surfaces (LB monolayers).^{12,32} Interestingly, these stars exhibit pH responsive self-assembly behavior owing to the ampholytic character of the diblock P2VP-*b*-PAA arms. A diversity of pH-induced self-assemblies was observed; from core-shell unimolecular micelles to multicore large compound micelles (LCM), worm-like micelles, network-like large assemblies and so on.^{12,32} A

^aDepartment of Chemical Engineering, University of Patras, 26504 Patras, Greece.

E-mail: ct@chemeng.upatras.gr; Fax: +30 2610 997266; Tel: +30 2610 969531

^bInstitute of Chemical Engineering Sciences ICE/HT-FORTH, P.O. Box 1414, 26504 Patras, Greece

† Electronic supplementary information (ESI) available: ¹H-NMR spectrum of S3422(V126-*b*-A119-*g*-N484)₂₂, autocorrelation functions of 0.2 wt% S339(V126-*b*-A69-*g*-N48_m)₉, aqueous solutions at pH 8 and at 25 °C or 45 °C, TEM images of 0.006 wt% S339(V126-*b*-A69-*g*-N48_{4.5})₉, aqueous solutions of pH 2.4 at 25 and 50 °C, sol-gel phase behavior upon heating from 25 °C to 50 °C at various pH of S3422(V136-*b*-A119-*g*-N48₄)₂₂ ($C_p = 3$ wt%). See DOI: 10.1039/c5py00393h

novelty these polymers can exhibit is their blocks' ability to be functionalized with various chemical species, thanks to the pendant pyridine and carboxyl groups along the arms, depending on the pH at which the functionalization is carried out. For example, it has been recently shown that either the polybase P2VP or the polyacid PAA of $PS_n(P2VP-b-PAA)_n$ can form ionic supramolecular complexes with oppositely charged surfactants through non-covalent interactions.⁶² Another prospect to enrich the self-assembly and application possibilities of these $PS_n(P2VP-b-PAA)_n$ star polymers would be a covalent functionalization to endow them with additional functionalities other than pH sensitivity (e.g. thermosensitivity).

Thus, in the present work we extend our recent study by designing novel multiarmed star quaterpolymers using the $PS_n(P2VP-b-PAA)_n$ stars as precursors to induce thermoresponsiveness by a simple grafting "onto" method through an amidation reaction between the carboxyls of the outer PAA segments and the amine group of PNIPAM-NH₂ short chains. The resulting $PS_n(P2VP-b-PAA-g-PNIPAM)_n$ star-graft quaterpolymers bear PS and poly(2-vinyl-pyridine)-*b*-poly(acrylic acid)-*g*-poly(*N*-isopropyl acrylamide) diblock-graft arms of different grafting density and number of arms. The self-organization behavior of these complex star macromolecules in aqueous media, either in dilute or concentrated solutions, was studied by various techniques. Thanks to the nature of the various segments, P2VP/PAA pH-responsive weak polyelectrolytes and thermo-responsive PNIPAM, these star-graft quaterpolymers exhibited complex solution behavior in aqueous media. Their intermolecular association, induced by heating, was affected by various factors concerning either the solution conditions of pH and ionic strength or the polymer architecture, namely number of arms and PNIPAM grafting density. More importantly, the star-grafts, designed herein, display additional self-assembly abilities as they can form thermoresponsive hydrogels based on transient networks.

2. Experimental part

2.1. Materials

Amine-terminated poly(*N*-isopropylacrylamide), PNIPAM-NH₂, of an average number molecular weight M_n 5500 g mol⁻¹, and

N-(3-dimethylaminopropyl)-*N'*-ethylcarbodiimide hydrochloride, EDC, were purchased from Aldrich.

2.2. Terpolymer synthesis and characterization

The synthesis of the $PS_n(P2VP-b-PAA)_n$ terpolymers has been described earlier.^{32d} Briefly, the $PS_n(P2VP-b-PtBA)_n$ heteroarm star terpolymer precursors were prepared *via* a one-pot/four-step sequential "living" anionic polymerization procedure (an extended "in-out" method). In the first step, the PS arms were prepared in THF, using *sec*-BuLi as the initiator. After the consumption of styrene, the 'living' PS chains were used to polymerize a small quantity of DVB, resulting in 'living' star-shaped polystyrene precursors (PS_n) bearing active sites in their PDVB core. The 'living' star polymers were used to initiate polymerization of 2VP, leading to the formation of a second generation of P2VP arms. Finally, the sites located at the end of the P2VP arms were used to polymerize tBA. In every step of the synthesis, sampling out was performed for the purpose of characterization. The $PS_n(P2VP-b-PAA)_n$ terpolymers were obtained after acidic hydrolysis of the PtBA blocks in 1,4-dioxane with a 6-fold excess of hydrochloric acid at 80 °C. The characterization results are presented in Table 1.

2.3. Synthesis and characterization of the graft quaterpolymers

For the preparation of the heteroarm $PS_n(P2VP-b-PAA-g-PNIPAM)_n$ star-graft quaterpolymers, the $PS_n(P2VP-b-PAA)_n$ star terpolymer was first dissolved in DMF, followed by slow addition of a sufficient quantity of 0.01 M of aqueous HCl solution until a 3/7 volume ratio of DMF/H₂O was achieved. The prepared solution was then dialyzed against 0.01 M HCl solution for 6 days to remove DMF, using a dialysis membrane (MWCO 12 000 Da). The resulting mother solution (pH 2) was again dialyzed against aqueous solutions of pH 8 for 4 days. At a second step, the PNIPAM-NH₂ chains were grafted onto the neutralized PAA of the terpolymer in aqueous solution and at room temperature, using EDC as a condensing agent. The mixture was left under gentle stirring for three days, while a quantity of 0.1 g of EDC was added daily. Then, the solution was dialyzed against H₂O to remove any non-grafted PNIPAM chains or excess of EDC, using a dialysis membrane (MWCO 25 000 Da). The final product was recovered by freeze drying.

Table 1 Molecular characteristics of the $PS_n(P2VP-b-PAA)_n$ star block terpolymers

Sample ^a	No. of arms ^b	PS		P2VP		PAA		Φ_{P2VP} ^f	M_w , total ^g (g mol ⁻¹)
		M_w ^c (g mol ⁻¹)	DP	M_w ^d (g mol ⁻¹)	DP	M_w ^e (g mol ⁻¹)	DP		
S33 ₉ (V126- <i>b</i> -A69) ₉	9.2	3400	33	13 200	126	4968	69	0.61	199 000
S34 ₂₂ (V136- <i>b</i> -A119) ₂₂	21.7	3500	34	14 300	136	8568	119	0.54	572 000

^a The numbers next to the letters denote the polymerization degree (DP) of each block while, the subscripts denote the number of arms. ^b Average number of arms of each kind by SLS. ^c By SEC. ^d Calculated by subtracting the M_w of the PS_n from that of PS_nP2VP_n and dividing by the number of arms n . ^e Calculated, by subtracting the M_w of the PS_nP2VP_n from that of $PS_n(P2VP-b-PtBA)_n$ and dividing by n , considering quantitative hydrolysis of tBA to AA. ^f P2VP weight fraction. ^g M_w of heteroarm star terpolymer (calculated).

2.4. Sample preparation

The experiments were conducted in H₂O using Millipore MILLIQ water. Contrary to the star terpolymer precursors, PS_n(P2VP-*b*-PAA)_n, which are initially insoluble in H₂O, all the PS_n(P2VP-*b*-PAA-*g*-PNIPAM)_n star-graft quarterpolymers are easily dissolved in H₂O. Thus, for all techniques, aqueous polymer solutions of various pH values were prepared by adding appropriate amounts of 0.1 M HCl or 0.1 M NaOH.

2.5. Turbidity

The optical density at 490 nm of polymer aqueous solutions (0.2 wt%) was measured using a double beam HITACHI U-2001 UV-Vis spectrophotometer equipped with a circulating water bath. The heating rate was regulated at 1 °C min⁻¹.

2.6. Static light scattering (SLS)

Light scattering measurements were carried out using a thermally regulated (±0.1 °C) spectro-goniometer, Model BI-200SM (Brookhaven), equipped with a He-Ne laser (632.8 nm).

2.7. Dynamic light scattering (DLS)

Autocorrelation functions $C(q,t)$ were measured with a Brookhaven BI-9000AT/Turbocorr digital correlator from a light source of He-Ne laser (632.8 nm). CONTIN analysis was performed through BI-DLSW software. The apparent hydrodynamic radius was determined *via* the Stokes-Einstein equation:

$$R_H = k_B T / 6\pi\eta D_{app}$$

where D_{app} is the diffusion coefficient, k_B is the Boltzmann constant and η is the viscosity of the solvent at absolute temperature T .

2.8. Electrophoresis

Zeta-potential measurements were carried out at 25 °C by means of a NanoZetasizer, Nano ZS Malvern apparatus. The excitation light source was a 4 mW He-Ne laser at 633 nm and the intensity of the scattered light was measured at 173°. A series of PS_n(P2VP-*b*-PAA-*g*-PNIPAM)_n solutions of different pH values ranging from 1 to 12 and at a concentration of 0.2 wt% were prepared in H₂O for the electrophoresis measurements.

2.9. Transmission electron microscopy (TEM)

TEM experiments were carried out using a JEM 2100 microscope operating at 200 kV. For TEM, very diluted aqueous polymer solutions (0.006 wt%) at different pH values were used. A drop of the dilute solution was deposited onto a carbon coated grid and allowed to evaporate at room temperature.

2.10. Rheology

The rheological measurements were carried out using a stress-controlled rheometer AR2000 (TA Instrument) equipped with a cone plate geometry (diameter 20 mm, cone angle 3°59'49", truncation 111 μm). The temperature was controlled using a Peltier plate connected to a Julabo AWC 100 system. A solvent

trap was used to minimize the changes in concentrations due to water evaporation. The experiments were performed in the linear viscoelastic regime established for every sample by a stress sweep at a frequency of 1 Hz. The star graft quarterpolymer produced low viscosity solutions at room temperature ($T < LCST$ of PNIPAM) at all pH values and gel formation was observed after heating above LCST. Thus, the temperature sweep experiments were carried out according to the following procedure. The vials with the aqueous solutions ($C_p = 3$ wt%, pH 2.5) were heated to 50 °C and at this temperature they were loaded on the Peltier plate (preheated at the same temperature). After equilibration at 50 °C for 15 min the temperature was decreased at a cooling rate of 1 °C min⁻¹ and G' and G'' (frequency: 1 Hz; strain: 6%) were recorded as a function of cooling the sample down to 20 °C.

3. Results and discussion

3.1. Synthesis and characterization of the star-graft quarterpolymers

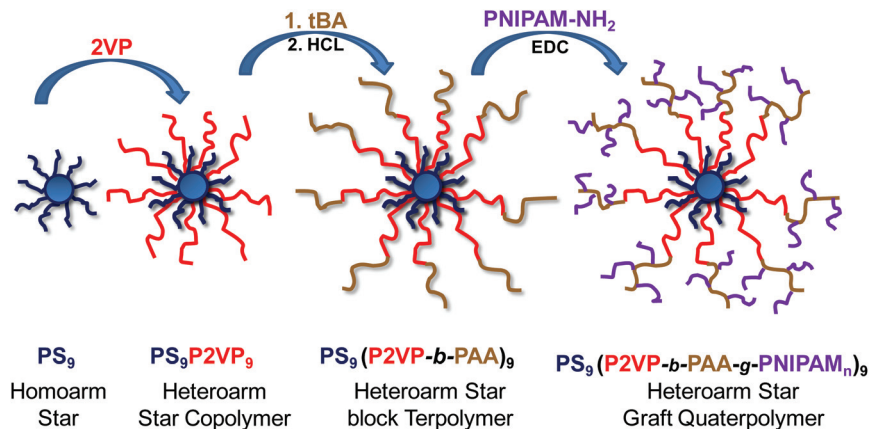
The synthesis of the star-graft quarterpolymers was carried out following a multi-pot reaction procedure as described in Scheme 1.

In the first pot, a heteroarm star block terpolymer was synthesized by “living” anionic polymerization according to the extended “in-out” method.⁴² This synthetic route has been described in a previous article and is briefly mentioned as a four-step procedure: (a) synthesis of the PS arms, (b) creation of PS_n star by using DVB, (c) growth of P2VP arms from the PDVB nodule (PS_nP2VP_n, *heteroarm star copolymer*) and (d) extension of the P2VP arms by adding tBA (PS_n(P2VP-*b*-PtBA)_n, *heteroarm star block terpolymer*). In the second pot, the PS_n(P2VP-*b*-PtBA)_n was subjected to acidic hydrolysis of the tBA segments yielding the PS_n(P2VP-*b*-PAA)_n. Lastly, in the third pot, the outer PAA segments were neutralized by NaOH, followed by a grafting “onto” procedure using amino terminated PNIPAM, in the presence of EDC as a condensing agent, yielding the PS_n(P2VP-*b*-PAA-*g*-PNIPAM)_n *heteroarm star-graft quarterpolymer*. Two PS_n(P2VP-*b*-PAA)_n star samples bearing 9 and 22 arms were used for further grafting with PNIPAM side chains.

The grafting density of the star-graft quarterpolymers, expressed as the average number of PNIPAM chains per PAA arms, was determined by ¹H-NMR in a mixture of deuterated solvents MeOD/CDCl₃ (3/2, v/v). The results on the chemical composition along with the estimated molecular weights of the polymers are compiled in Table 2.

3.2. pH dependent aqueous solution properties

Electrophoresis experiments were first performed in order to explore the charge properties of the S33₉(V126-*b*-A69-*g*-N48_m)₉ copolymers. For the zeta potential measurements, a series of S33₉(V126-*b*-A69-*g*-N48_m)₉ aqueous solutions, at different pH values ranging from 1 to 12 and at a concentration of 0.2 wt%, were prepared and the results are presented in Fig. 1. For the



Scheme 1 Synthetic route for the preparation of heteroarm star-graft quarterpolymers.

Table 2 Characterization data of the heteroarm star-graft quarterpolymers

Polymer topology ^a	Number of 2VP-PAA arms ^b	M_w of star precursor ^c (g mol ⁻¹)	M_w of star-graft quarterpolymer ^d (g mol ⁻¹)	Average PNIPAM chains per PAA arm ^e	PNIPAM weight fraction ^e
S33 ₉ (V126- <i>b</i> -A69- <i>g</i> -N48 _{3,4}) ₉	9.2	199 000	372 558	3.43	0.46
S33 ₉ (V126- <i>b</i> -A69- <i>g</i> -N48 _{4,5}) ₉			426 194	4.49	0.53
S33 ₉ (V126- <i>b</i> -A69- <i>g</i> -N48 ₁₁) ₉			759 648	11.08	0.74
S34 ₂₂ (V136- <i>b</i> -A119- <i>g</i> -N48 ₄) ₂₂	21.7	572 000	1 049 400	4.00	0.45

^a The numbers next to the letters denote the polymerization degree (DP) of each block while, the subscripts denote the number of arms and/or grafts per arm. ^b By light scattering of PS_n star precursor. ^c By light scattering of heteroarm PS_n(P2VP-*b*-PAA)_n and assuming quantitative deprotection of tBA moieties. ^d Calculated from M_w of PS_n(P2VP-*b*-PAA)_n precursor and PNIPAM weight fraction. ^e By ¹H-NMR.

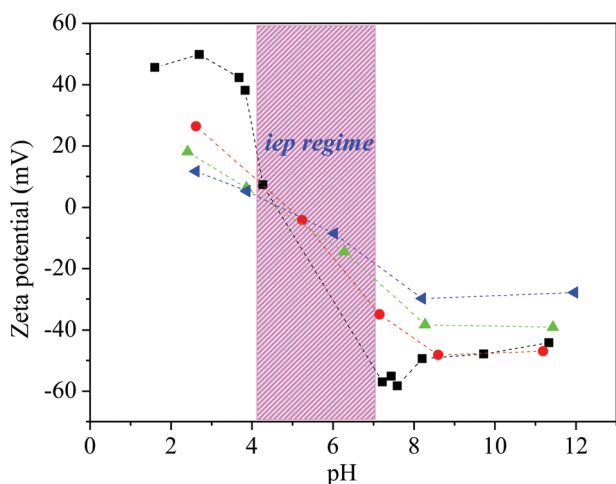


Fig. 1 Zeta potential as a function of pH of 0.2 wt% S33₉(V126-*b*-A69-*g*-N48_{3,4})₉ (●), S33₉(V126-*b*-A69-*g*-N48_{4,5})₉ (▲) and S33₉(V126-*b*-A69-*g*-N48₁₁)₉ (◀) aqueous solutions. The marked region denotes the precipitation regime for the non-grafted S33₉(V126-*b*-A69)₉ terpolymer precursor (■).

sake of comparison, the charge state of the star terpolymer precursor S33₉(V126-*b*-A69)₉ is also shown in Fig. 1. It should be noted that the precursor S33₉(V126-*b*-A69)₉ is not easily dis-

solved in water. For this reason, it was first dissolved in DMF, followed by slow addition of a sufficient quantity of 0.01 M aqueous HCl solution until a DMF/H₂O volume ratio 3/7 was achieved and then dialysis was done against 0.01 M HCl solution for 6 days using a dialysis membrane (MWCO 12 000 Da) in order to remove DMF.

At low pH values (pH < 4), positive charges predominate due to the protonation of the P2VP segments that behave like a cationic polyelectrolyte, while at the same time the PAA blocks are mainly neutral. For intermediate pH values (4 < pH < 7) the zeta potential takes values close to zero as electrostatic interactions of the oppositely charged PAA and P2VP segments take place. Furthermore, in the case of the precursor, at this pH region (isoelectric point regime, iep) where the P2VP segments progressively become hydrophobic, a two-phase region, in which the terpolymer precipitated, was observed and therefore zeta potential could not be determined. Upon further increasing pH (pH > 7), the net charge of the polymer solution switched from zero to negative values due to the strong ionization of the PAA segments. In contrast, as can be clearly seen, the polymer remained always water soluble in the case of the star graft quarterpolymers, S33₉(V126-*b*-A69-*g*-N48_m)₉, and exhibited zero z-potential in the vicinity of pH 5 (iep). Apparently, the addition of the hydrophilic PNIPAM side chains on the PAA segments enhances the solubility of the copolymers even at the iep.

The different z -potential values of the polymer solutions at $\text{pH} > 7$ could be correlated to the grafting density of the PNIPAM chains. For $\text{S33}_9(\text{V126-}b\text{-A69-}g\text{-N48}_{3,4})_9$, where the average number of the PNIPAM pendant chains per arm is the lowest, the net charge took the more negative values, close to that of the star precursor without PNIPAM side chains. As the grafting density of PNIPAM chains increased, the number of negatively charged AA moieties at the surface of the star polymer decreased, due to the increasing amidation of the $-\text{COOH}$ moieties and likely to the PNIPAM hindering effects, thus resulting in lower negative z -potential values. An analogous trend was observed in the low pH region where the positive z -potential values decreased with the grafting density.

3.3. Thermo-responsiveness

In Fig. 2a, photos of aqueous $\text{S33}_9(\text{V126-}b\text{-A69-}g\text{-N48}_{4,5})_9$ solutions of a concentration of 0.2 wt% at acidic (pH 2), near isoelectric point (pH 6) and under basic (pH 8) conditions and at 25 °C are presented. As can be seen, the $\text{S33}_9(\text{V126-}b\text{-A69-}g\text{-N48}_{4,5})_9$ solutions are transparent at all pH conditions and no precipitation was observed, even at pH 6 where the $\text{S33}_9(\text{V126-}b\text{-A69})_9$ precursor becomes water insoluble. This behavior confirms the fact that introduction of the PNIPAM chains on the PAA segments augments the water solubility of the system. While at room temperature the PNIPAM chains improve the stability of the polymers in the aqueous solution, it is expected that at higher temperatures the hydrophobicity of the polymers will be enhanced remarkably due to the hydrophobic transformation of PNIPAM above its LCST. Thus, we investigated subsequently the thermal response of $\text{S33}_9(\text{V126-}b\text{-A69-}g\text{-N48}_{4,5})_9$ polymer solutions by heating at 50 °C, which is considerably higher than the well known LCST (*ca.* 32 °C) of the PNIPAM homopolymer (Fig. 2b). At pH 2 and pH 6, the polymer solutions became turbid while, at pH 8 the solution remained transparent. This could be explained as follows: at low pH (pH 2), the outer PAA segments are neutral and the PNIPAM chains become completely hydrophobic. Nevertheless, the polymer does not precipitate as the P2VP segments are highly protonated, stabilizing the polymer in water. At pH 6 (vicinity of iep) where electrostatic interactions between the negatively charged PAA and some remaining positively charged 2VP groups (the majority have become hydrophobic) take place, the hydrophobic content of the polymer was highly

increased. Surprisingly, even in this case, precipitation was not observed. Finally, at pH 8 where the P2VP segments are totally hydrophobic and although the PNIPAM grafting chains became hydrophobic too, no turbidity was observed owing to the high solubility of the fully ionized PAA segments.

The thermoresponsive behavior of the star-graft $\text{S33}_9(\text{V126-}b\text{-A69-}g\text{-N48}_m)_9$ quarterpolymers was also monitored through turbidity and SLS. In Fig. 3, the temperature dependence of the optical density at 490 nm (Fig. 3a) and the light scattering intensity at 90°, I , (Fig. 3b) of 0.2 wt% $\text{S33}_9(\text{V126-}b\text{-A69-}g\text{-N48}_{4,5})_9$ aqueous solutions at various pH are presented. As seen in Fig. 3a, since the polymers are completely dissolved in water at all pHs, fully transparent solutions were obtained at low temperatures. In contrast, upon heating above the LCST of the thermosensitive PNIPAM side chains and particularly above $T = 35$ °C, a dramatic increase of the optical density was observed for the samples at pH 2.4, 5 and 6, showing the self-association of the star-graft quarterpolymer as PNIPAM became hydrophobic, in accordance with the optical observation in Fig. 2. The temperature above which the optical density of the polymer solution increases abruptly is denoted as the cloud point temperature, T_{cp} .

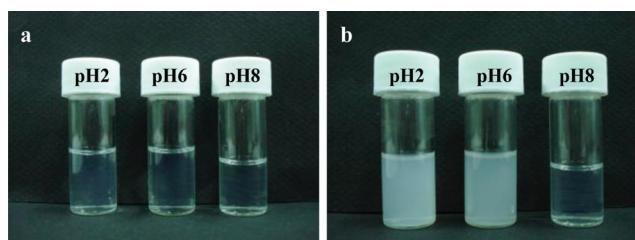


Fig. 2 Photograph of 0.2 wt% $\text{S33}_9(\text{V126-}b\text{-A69-}g\text{-N48}_{4,5})_9$ aqueous solutions of different pH values at (a) 25 °C and (b) 50 °C.

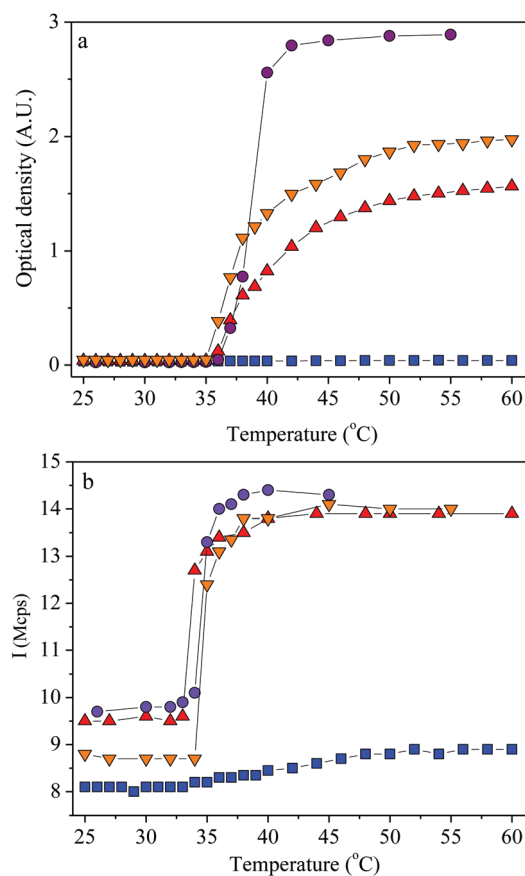


Fig. 3 Temperature dependence of the optical density (a) and the light scattering intensity at 90° (b) of 0.2 wt% $\text{S33}_9(\text{V126-}b\text{-A69-}g\text{-N48}_{4,5})_9$ salt free aqueous solutions at pH 2.4 (▲), pH 5 (●), pH 6 (▼) and pH 8 (■). The lines are a guide for the eyes.

More interestingly, one can notice that the thermal behavior of the solutions is pH dependent. It seems that the highest and lowest turbidity were observed at pH 5 and pH 2.4, respectively, while intermediate behavior was observed at pH 6. At pH 2.4, the protonated and highly stretched P2VP segments stabilized very well the polymer in water and thus the turbidity was less pronounced. At pH 5 and 6 (iep region), a more pronounced turbidity was observed while precipitation was avoided, as should be expected. Indeed, in this pH/temperature state, the polymers should exhibit the most hydrophobic character as the oppositely charged P2VP and PAA groups interact electrostatically with each other (the net charge of the system approaches zero, Fig. 1) and the PNIPAM chains become hydrophobic. It seems that the electrostatic interactions among the oppositely charged moieties were prevented due to steric hindrance effects exerted by the PNIPAM grafting chains, thus stabilizing the system.

Unexpected behavior was observed at pH 8, at which the copolymer solution remained transparent and water soluble for the entire temperature range studied ($25\text{ °C} < T < 60\text{ °C}$). This should be attributed to the high hydrophilicity of the fully ionized PAA outer segments of the star molecule. More importantly, the intermolecular hydrophobic interactions of PNIPAM grafts seem to be avoided, preventing turbidity.

Additional and more sensitive information on the association behavior of the polymer solutions could be obtained using SLS. As shown in Fig. 3b, at low temperatures, the light scattering intensity at 90° , I , is relatively low for all polymer solutions, likely because no polymer association occurs due to the star macromolecular architecture.^{46b,d,63} Upon heating the solution above a critical temperature termed association temperature (T_{ass}) which is the temperature above which the light scattering intensity increases abruptly, I rose dramatically for the solutions at pH 2.4, 5 and 6, revealing thermo-induced hydrophobic association, in accordance with the turbidity results. However, slightly lower T_{ass} s (ca. at 33 °C for pH 2.4 and 34 °C for pH 5 and 6) were observed regarding the corresponding T_{cps} ($35\text{--}36\text{ °C}$), due to the higher ability of light scattering to detect associates of lower sizes than UV-Vis absorption spectroscopy. In the case of pH 8, a slight, non-abrupt increase of I occurred above 34 °C , revealing a weak thermo-responsiveness not observable by turbidimetry measurements (Fig. 3a), implying mainly intramolecular hydrophobic interactions. This unexpected behaviour could be ascribed to the high degree of ionization of the PAA “backbone” segments in the outer periphery of the star molecules, the repulsive interactions of which might prevent the intermolecular thermo-association of the hydrophobic PNIPAM stickers.

In order to explore the influence of PNIPAM grafting density of the star-grafts on the temperature responsive association behavior, SLS was also utilized for the two other samples of the same series (grafting from the same star precursor) at the different pH regimes. In Fig. 4, the normalized light scattering intensity at 90° , of 0.2 wt% $S33_9(V126\text{-}b\text{-}A69\text{-}g\text{-}N48_m)_9$ star-graft aqueous solutions are demonstrated *versus* temperature at various pH. At low pH (Fig. 4a), the behavior of

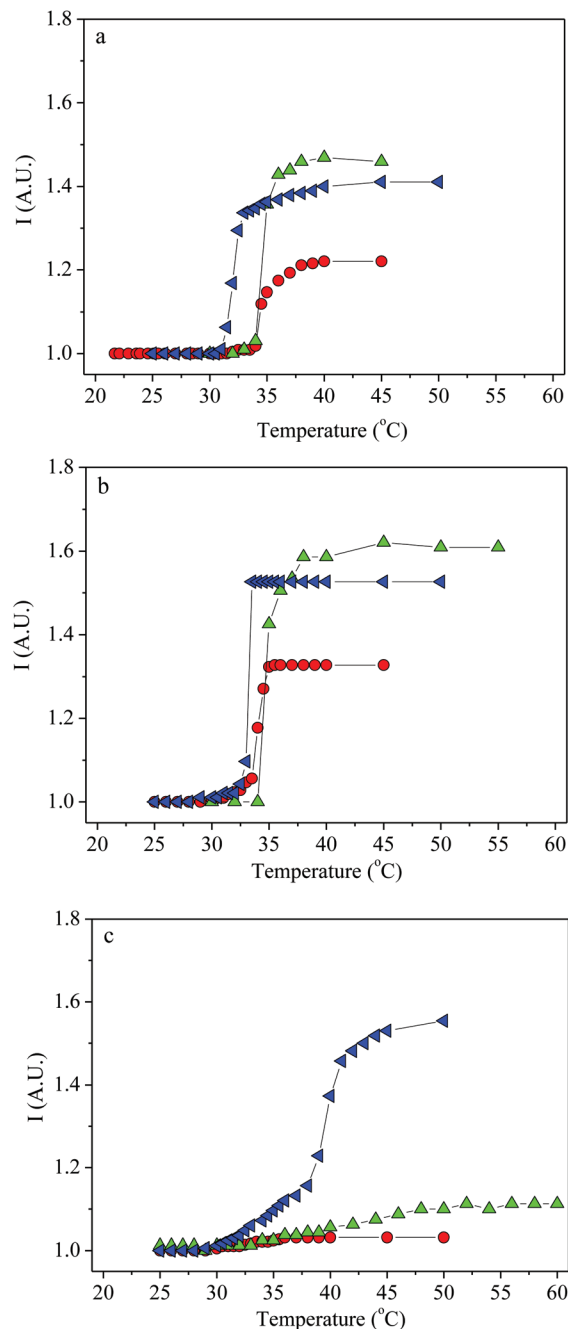


Fig. 4 Temperature dependence of the normalized light scattering intensity at 90° of salt free aqueous solutions of 0.2 wt% $S33_9(V126\text{-}b\text{-}A69\text{-}g\text{-}N48_{3,4})_9$ (●), $S33_9(V126\text{-}b\text{-}A69\text{-}g\text{-}N48_{4,5})_9$ (▲) and $S33_9(V126\text{-}b\text{-}A69\text{-}g\text{-}N48_{11})_9$ (◀) at (a) pH 2.4, (b) pH 5 and (c) pH 8. The lines are a guide for the eyes.

$S33_9(V126\text{-}b\text{-}A69\text{-}g\text{-}N48_{3,4})_9$ is similar to that of $S33_9(V126\text{-}b\text{-}A69\text{-}g\text{-}N48_{4,5})_9$, since both polymers show the same T_{ass} at 34 °C . On the other hand, the $S33_9(V126\text{-}b\text{-}A69\text{-}g\text{-}N48_{11})_9$ sample exhibited a lower $T_{\text{ass}} \sim 31\text{ °C}$, which should be attributed to the considerably higher PNIPAM grafting density that favored interstar association. At pH 5, all star-grafts exhibited

the same behavior with slightly different T_{ass} between 33 and 34 °C (Fig. 4b).

Finally, under basic conditions (pH 8, Fig. 4c), while the thermosensitivity of the $S33_9(V126-b-A69-g-N48_{3,4})_9$ and $S33_9(V126-b-A69-g-N48_{4,5})_9$ solutions remained very weak with I being practically unaffected upon heating, the $S33_9(V126-b-A69-g-N48_{11})_9$ solutions showed different and unusual behavior. The intensity I of the sample remained constant for low temperatures and increased gradually above 31 °C up to 38 °C, leading eventually to an abrupt increase at $T > 38$ °C. This two-step thermoresponsive behavior might be the result of a synergistic effect involving two factors, namely electrostatic repulsive interactions (controlled by pH) and macromolecular topology which in this case is the highest grafting density of PNIPAM chains. The enhancement of grafting density decreases the repulsive interactions (lowering the AA moieties) while it increases the number of hydrophobic stickers. Consequently, the higher PNIPAM grafting density allowed the appearance of the thermo-induced intermolecular association even under basic conditions.

As known, the LCST of thermosensitive polymers is affected by the ionic strength (salting out effect).⁶⁴ Taking this into consideration, it was anticipated that the association temperature of the quarterpolymers should be sensitive to the presence of salts as well. Thus, SLS measurements were conducted at constant pH and various concentrations of NaCl. In Fig. 5, the temperature dependence of the normalized light scattering intensities at 90° of aqueous solutions of 0.2 wt% $S33_9(V126-b-A69-g-N48_{3,4})_9$ (Fig. 5a), $S33_9(V126-b-A69-g-N48_{4,5})_9$ (Fig. 5b) and $S33_9(V126-b-A69-g-N48_{11})_9$ (Fig. 5c) measured at pH 5 with 0 M, 0.1 M and 0.3 M NaCl are presented.

As can be observed, T_{ass} was shifted to a lower temperature upon increasing ionic strength in all three samples, as expected. It also seems that the PNIPAM grafting density influences the magnitude of T_{ass} -shift as the $S33_9(V126-b-A69-g-N48_{3,4})_9$, having the lowest grafting density, exhibited the most notable T_{ass} decrease from 33 to 27 °C, about 6 degrees lower compared to the salt free solution. Provided that the positively charged 2VP and the negatively charged AA moieties interact with each other at pH 5 (iep), the increase of ionic strength should affect also these attractive interactions. This probably influences the interstar association as it is manifested in the magnitude of light scattering intensity. Indeed, this effect is clear for the $S33_9(V126-b-A69-g-N48_{4,5})_9$ sample in Fig. 5b, where the plateau value of I at high temperatures increased parallel to the T_{ass} shift upon increasing the salt concentration. However, this trend is differentiated in the other two star-grafts showing again the influence of the grafting density. Therefore, synergistic effects on the association behavior of the star-graft quarterpolymers by varying the ionic strength were again observed.

To have a better insight of the effect of heating on the self-organization of the star-graft quarterpolymers in dilute aqueous solutions, preliminary DLS and TEM experiments were conducted at low pH for the $S33_9(V126-b-A69-g-N48_{4,5})_9$ star-graft quarterpolymer. In Fig. 6a and c, the autocorrelation

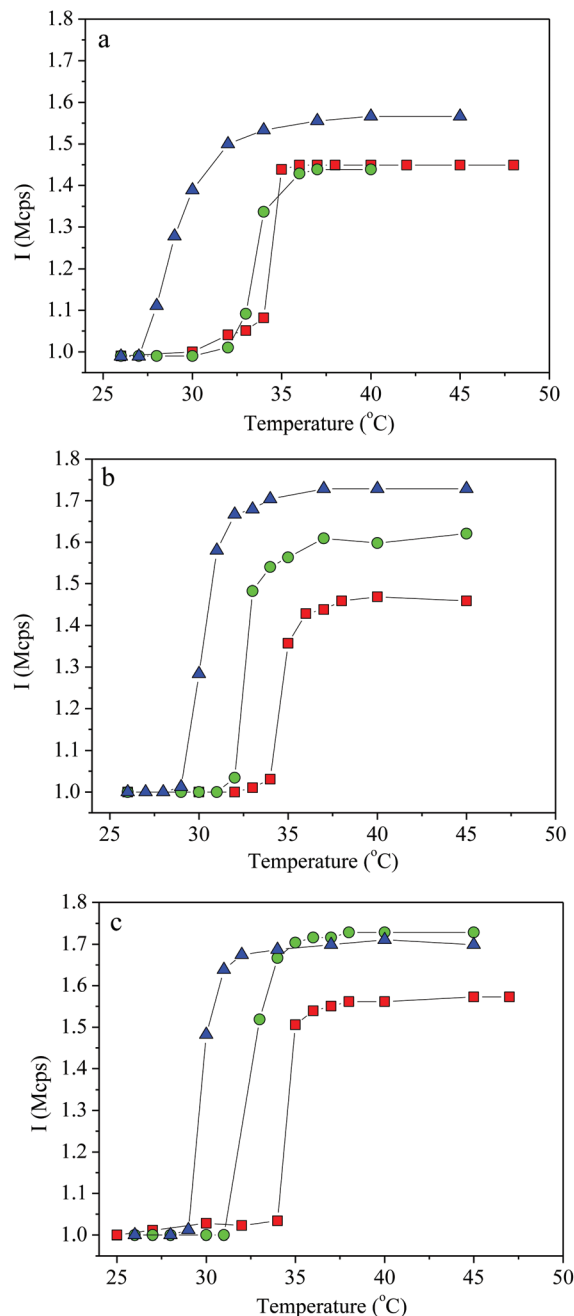


Fig. 5 Temperature dependence of the normalized light scattering intensity at 90° of 0.2 wt% $S33_9(V126-b-A69-g-N48_{3,4})_9$ (a) $S33_9(V126-b-A69-g-N48_{4,5})_9$ (b) and $S33_9(V126-b-A69-g-N48_{11})_9$ (c) aqueous solutions at pH 5 without NaCl (■) or with 0.1 M NaCl (●) and 0.3 M NaCl (▲). The lines are a guide for the eyes.

functions and the corresponding size distributions, respectively, deduced by CONTIN analysis are presented, below and above the association temperature (33 °C from Fig. 3b) of the 0.2 wt% star-graft salt free aqueous solution. It is obvious that the size of the nanostructures increased from about 60 nm in diameter to 200 nm, revealing an interstar association upon heating the solutions. To better understand the association

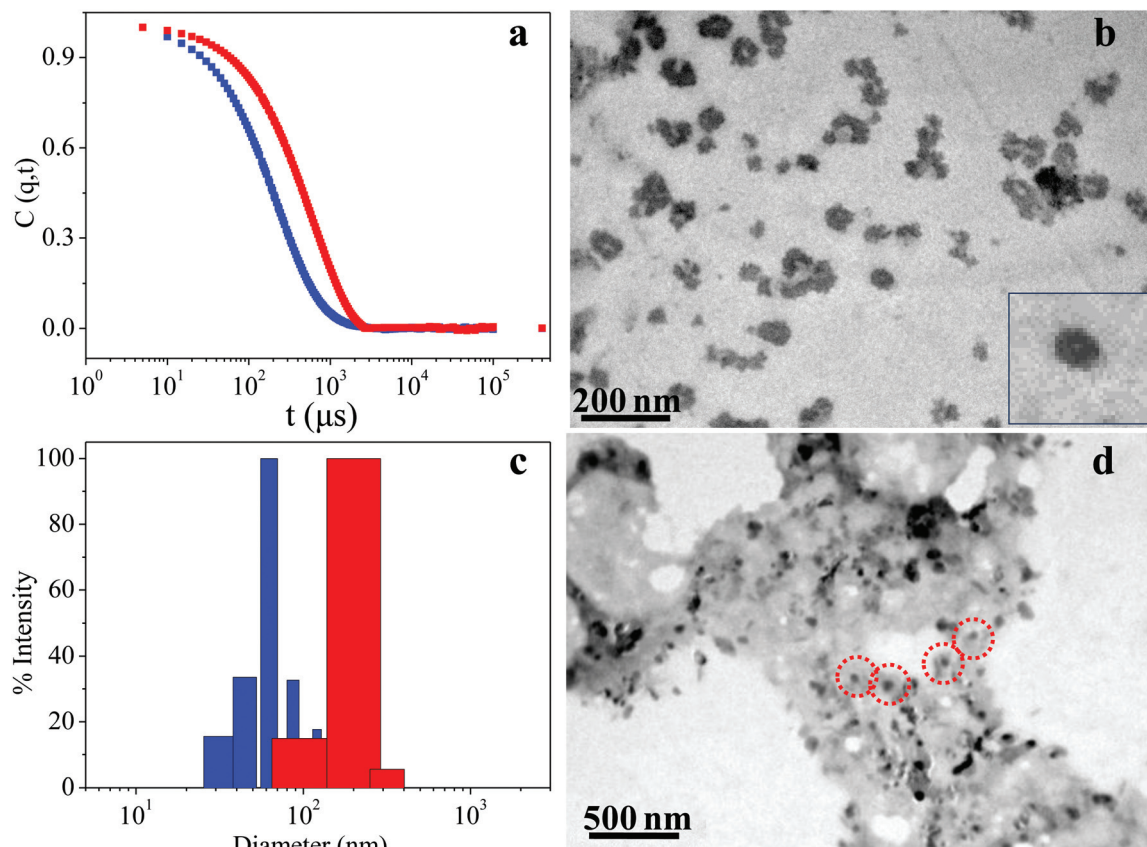


Fig. 6 Autocorrelation function (a) and intensity weighted hydrodynamic size (c) of 0.2 wt% S33₉(V126-*b*-A69-*g*-N48_{4.5})₉ aqueous solutions of pH 2.4 at 25 °C (blue color) and 50 °C (red color). TEM images of 0.006 wt% S33₉(V126-*b*-A69-*g*-N48_{4.5})₉ aqueous solutions of pH 2.4 at 25 °C (b) and 50 °C (d). Inset of (b): zoom of a core-shell particle; the associated spherical micelles have been marked by red circles in (d).

procedure, TEM images of nanostructures embedded on carbon substrates from 0.006 wt% polymer aqueous solutions of pH 2.4 at 25 °C and at 50 °C are also displayed (Fig. 6 and S3†). At room temperature, spherical nano-objects were observed with a size varying from ~45–80 nm in diameter (Fig. 6b), in good accordance with the DLS results. It is likely that these nano-objects are unimolecular micelles or at least associates of very low aggregation number as the star architecture dictates.^{46b,d,63} Upon heating above the T_{ass} of the solution (Fig. 6d), intermicellar aggregation was observed, due to the hydrophobic PNIPAM side chain intermolecular association, forming large sized aggregates comprising spherical micelles (Fig. 6d, inset). Because of the preparation method (increasing concentration upon solvent evaporation), this image shows a tendency towards a network-like structure, which is confirmed in concentrated solutions in the next section.

3.4. Sol-gel phase behavior

Preliminary investigations were also undertaken to explore the gelation ability of these multifunctional star-graft quarterpolymers in more concentrated aqueous solutions. In particular, we were interested in seeing whether sol-gel transitions could occur upon heating the solutions in pH controlled environ-

ments. In Fig. 7, digital photos of a series of 3 wt% S33₉(V126-*b*-A69-*g*-N48_{3.4})₉ aqueous solutions at different pH and equilibrated in two temperatures below and above the association temperature (as observed in Fig. 4) of the star-grafts are demonstrated.

At 25 °C, bluish turbid solutions were observed in all cases showing an aggregation tendency of the star-graft quarterpolymers at elevated concentrations. It is also observed that at pH 2 the solution is viscous, which means that at this concentration the star-graft macromolecules seem to interact intermolecularly, but they are still below a percolation concentration. Upon heating at 50 °C, opaque free supporting gels were observed at different pH windows, that are at low pH (pH < 2.5) as well as at pH in the vicinity of the isoelectric point (pH 5, see Fig. 1) of the macromolecule. More importantly, at pH 7.4 (physiological pH) the solution remained intact, in agreement with the weak thermoassociativity observed at lower concentrations (Fig. 4c). Therefore, it is obvious that pH, controlling the degree of ionization of the P2VP and PAA segments, affects remarkably the gelation efficiency of these thermo-responsive macromolecules.

To explore the possible influence of the grafting density of PNIPAM, the same experiments were conducted for the three

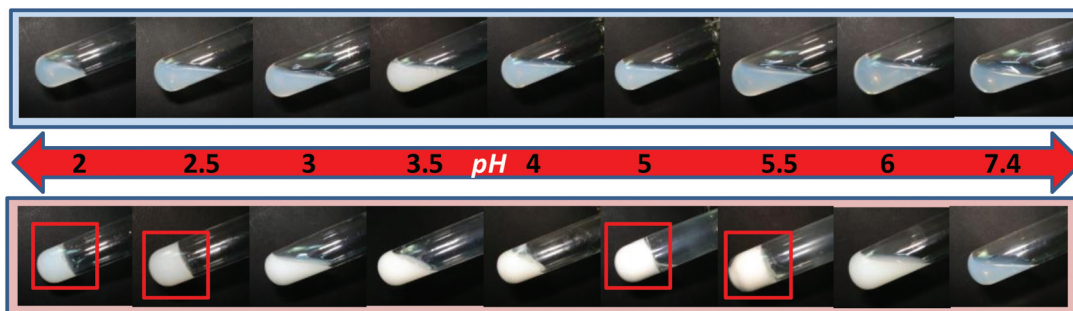


Fig. 7 Sol-gel phase behavior upon heating from 25 °C (upper line) to 50 °C (lower line) at various pH of $S33_9(V126-b-A69-g-N48_{3.4})_9$ ($C_p = 3$ wt%).

samples of the $S33_9(V126-b-A69-g-N48_m)_9$ series. Fig. 8 demonstrates the digital photos obtained from the polymer solutions after equilibration at 50 °C. It can be directly deduced that the PNIPAM grafting density is another factor that affects the thermo-induced gelation behavior of the system.

Although the gel phase appeared again at low pH and in the isoelectric region, significant differences can be observed among the different samples. Firstly, the gelation efficiency was expanded to pH 3 as the grafting density increases from $S33_9(V126-b-A69-g-N48_{3.4})_9$ to $S33_9(V126-b-A69-g-N48_{11})_9$. More interesting effects were observed in the isoelectric regime. A clear gel phase appeared at pH 4 for the highest grafting density $S33_9(V126-b-A69-g-N48_{11})_9$ sample. More importantly, phase separation (syneresis) occurred with increasing grafting density at pH 5 and 5.5 that is more pronounced in pH 5.5. Lastly, although a milky solution appeared at pH 7.4 in $S33_9(V126-b-A69-g-N48_{11})_9$, gelation was not observed.

Finally, the same experiment as above was performed for the $S34_{22}(V136-b-A119-g-N48_4)_{22}$ sample which bears 22 arms, in an attempt to explore the effect of the number of arms on the sol/gel phase behavior at various pH windows. Again upon heating, opaque gel and turbid sol were observed in low and

high pH respectively (Fig. S3†). However, comparing the overall behavior of the 22 armed star-grafts with those of 9 armed counterpart with about the same grafting density (SG1–SG2, Fig. 8) we did not observe gelation at intermediate pH (vicinity of iep) but precipitation. This significant different response indicates that the number of arms constitutes an additional factor which influences the solution behavior of these star-graft macromolecules.

Preliminary oscillatory rheological experiments were conducted subsequently to determine the gel to sol transition in the low pH window. The samples were loaded at 50 °C on the rheometer, and after equilibration a temperature ramp was performed from 50 °C down to 20 °C at a cooling rate of 1 °C min^{-1} . In Fig. 9, the elastic, G' , and loss modulus, G'' obtained in the linear viscoelastic regime and at constant frequency of 1 Hz, are plotted as a function of temperature. In all three samples, the elastic modulus predominated over the loss modulus at high temperatures and remained constant, in accordance with the free supporting gel behavior observed in Fig. 8. Below *ca.* 33 °C, the moduli began to decrease smoothly and below *ca.* 28 °C they decreased steeply several orders of magnitude, followed by a crossover of G'/G'' at about 25 °C

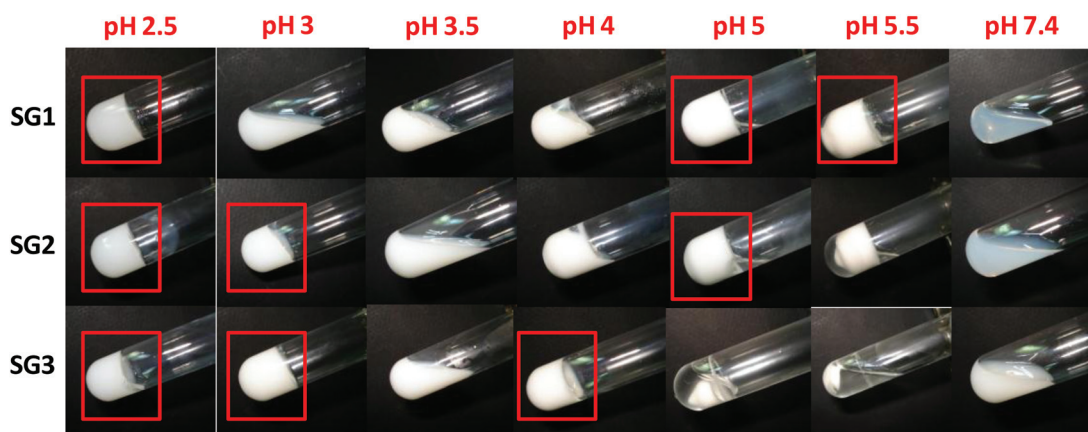


Fig. 8 Effect of grafting density in phase behavior of star-graft quarterpolymers above the LCST of the PNIPAM grafted chains (50 °C) at various pH ($C_p = 3$ wt%): $S33_9(V126-b-A69-g-N48_{3.4})_9$ (SG1), $S33_9(V126-b-A69-g-N48_{4.5})_9$ (SG2), $S33_9(V126-b-A69-g-N48_{11})_9$ (SG3).

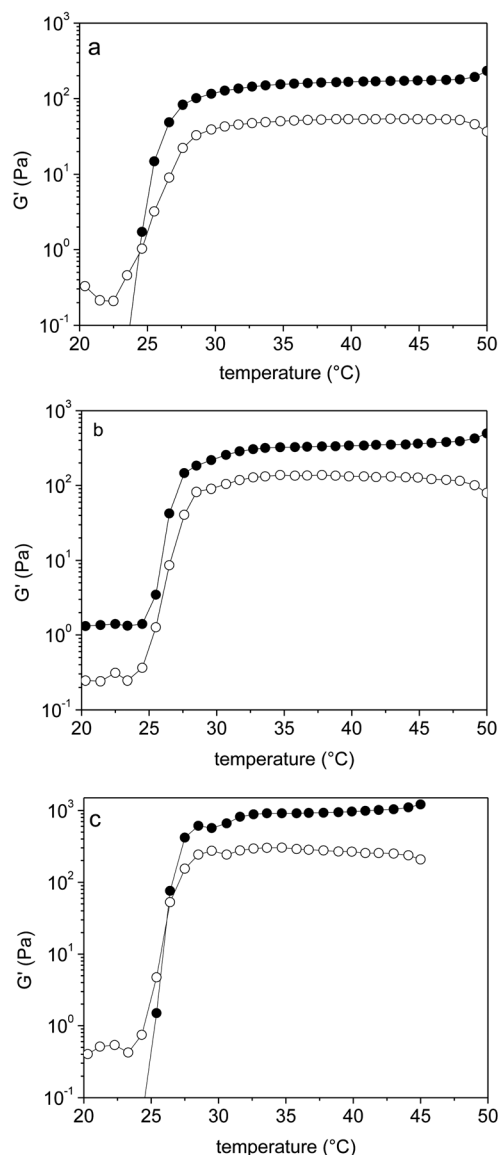


Fig. 9 Viscoelastic properties of 3 wt% aqueous solutions of $S33_9(V126-b-A69-g-N48_{3.4})_9$ (a), $S33_9(V126-b-A69-g-N48_{4.5})_9$ (b) and $S33_9(V126-b-A69-g-N48_{11})_9$ (c) star graft copolymers at pH 2.5 as a function of temperature measured during a cooling procedure.

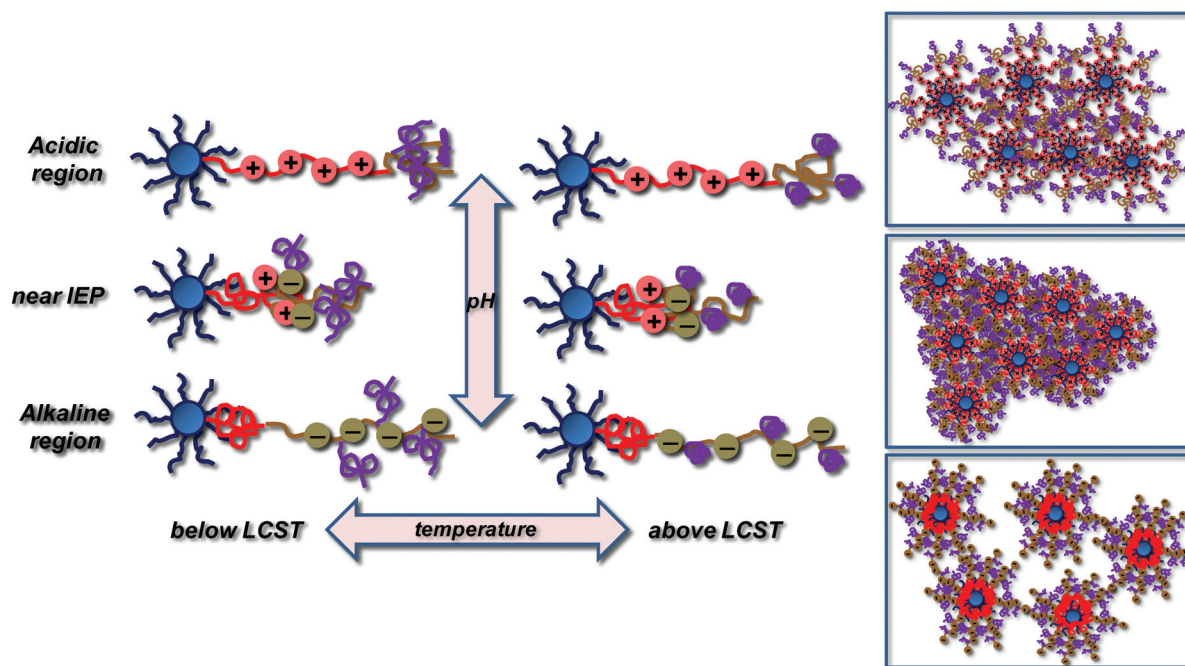
revealing a gel to sol transition. The latter was not observed for the $S33_9(V126-b-A69-g-N48_{4.5})_9$ sample in which the G' continued to prevail over G'' but at considerable lower values (of the order of 1 Pa), indicating a viscous sol behavior, in accordance with the optical observations. It is worth mentioning that the gel to sol transition is observed as expected at temperatures several degrees lower than the T_{ass} of star-grafts determined at low concentrations (Fig. 4a) since it is known that T_{ass} decreases with increasing polymer concentration. Although the transition temperature was nearly the same for all samples, the moduli at the gel phase were remarkably influenced by the PNIPAM grafting density. Particularly, the elastic modulus increased from 160 Pa in $S33_9(V126-b-A69-g-N48_{3.4})_9$

to 925 Pa in $S33_9(V126-b-A69-g-N48_{11})_9$, which is about 6 times higher for about 3 times more PNIPAM chains per arm, indicating that the number density of the elastic chains of the network (bridging two stars) is augmented remarkably due to the increasing probability of PNIPAM intermolecular hydrophobic attractions.

The appearance of free supporting gels upon heating should be attributed to the ability of these complex macromolecules to generate a three dimensional transient network. The driving interactions, induced at high temperatures, which are expected to function towards network formation are hydrophobic interactions exerted by the PNIPAM chains (stickers) grafted on the outer PAA blocks of the P2VP-PAA arms of the star polymer. However, secondary interactions of electrostatic nature, attributed to the positively charged protonated P2VP moieties (at low pH) and the negatively charged deprotonated PAA (at high pH), as well as H-bonding among the non-protonated P2VP (above pH 4) and/or NIPAM and the AA moieties (below pH 3) also seem to influence the network formation, affecting remarkably the thermo-induced gelation ability of these star-graft macromolecules.

In Scheme 2, the conformation of the various segments of the P2VP-*b*-PAA-*g*-PNIPAM arms at different conditions have been drawn in an attempt to better understand the influence on the arm conformation of the various interactions that interplay among the segments under specific pH and temperature conditions. At low pH (acidic regime), the inner P2VP segments are positively charged, adopting more or less stretched conformations due to the repulsive interactions along the arms. On the other hand, the protonated PAA segments should form complexes with the PNIPAM grafting chains due to H-bonding.⁶⁵ The fact that the z-potential is lower regarding the non-grafted star precursor and decreases with the grafting density (Fig. 1) shows a shielding effect resulting from these outer intramolecular PAA/PNIPAM polymer complexes. This physical picture should explain the stronger tendency for inter-star association through the outer PAA/PNIPAM complexes already appearing at low temperature (viscous solutions). Upon increasing temperature above the LCST of PNIPAM grafts, H-bonding weakens and the PNIPAM segments interact hydrophobically and intermolecularly, leading to a 3D network. This is consistent with the dramatic increase of the elastic modulus which also increases with increasing PNIPAM grafting density, approaching 10^3 Pa for $S33_9(V126-b-A69-g-N48_{11})_9$ (Fig. 9).

At high pH (alkaline region), the P2VP segments become hydrophobic and tend to collapse close to the PS/PDVB core of the star. The outer PAA segments are now deprotonated, transformed to strong negatively charged polyelectrolytes, while the H-bonding with the PNIPAM grafts has been entirely suppressed. The hydrophobic content of the star-graft polymer has thus been considerably increased and probably leads to interstar association phenomena, as observed at elevated concentrations and low temperature (bluish solutions, Fig. 7). However, upon heating the sample above the LCST of PNIPAM grafting segments, gelation was not observed even in the sample with the highest grafting density, $S33_9(V126-b-A69-g-$



Scheme 2 Schematic representation of conformational changes induced by pH and temperature variation of the $(\text{P2VP-}b\text{-PAA-g-PNIPAM})_n$ arms of the heteroarm star graft quarterpolymers bearing 9 arms (for the sake of clarity only one $\text{P2VP-}b\text{-PAA-g-PNIPAM}$ arm per star is depicted). In the right panels, schematics of the corresponding interstar association, induced by heating, are also demonstrated. Note that in alkaline solutions, the electrostatic repulsive interactions prevent extensive association.

$\text{N48}_{11})_9$. A plausible cause of the non-formation of a 3D network could be attributed mainly to a significant decrease of the effective arm length. This occurs because the arm length is mainly determined from the neutralized PANA ($\text{DP}_n = 69$) segment, since P2VP ($\text{DP}_n = 126$) has collapsed. In addition, the degree of ionization decreases with the grafting density enhancement, as more negatively charged moieties are replaced by the PNIPAM grafts (decrease of the negative z -potential, Fig. 1). The latter implies weakening of the repulsive interaction along the arms, resulting in lower chain stretching, which in addition favors intra-star PNIPAM hydrophobic interactions. This was verified by DLS, where a decrease of the size of the micelles was observed upon heating for $\text{S33}_9(\text{V126-}b\text{-A69-g-N48}_{3,4})_9$ and $\text{S33}_9(\text{V126-}b\text{-A69-g-N48}_{4,5})_9$ (Fig. S2†). However, for the $\text{S33}_9(\text{V126-}b\text{-A69-g-N48}_{11})_9$ sample of the highest grafting density, interstar aggregation was observed, in good agreement with the turbidity augmentation (Fig. 8). Nevertheless, it seems that intermolecular repulsive interactions might oppose the extended hydrophobic star aggregation, which prevents the necessary surpassing of the percolation threshold for the network formation, at least in the concentration range investigated.

Lastly, at intermediate pH (iep region), the system is more complicated since all kinds of interactions come into play, *i.e.* electrostatic interaction among the opposite charges and H-bonding between AA and 2VP or NIPAM moieties. We should recall that at this pH window (Fig. 1) the precursor star precipitates while the presence of PNIPAM grafts on the outer

PAA segments preserves water solubility. Surprisingly, the star-graft quarterpolymer, instead of precipitating upon heating (PNIPAM hydrophobic state), forms a gel phase [$\text{S33}_9(\text{V126-}b\text{-A69-g-N48}_{3,4})_9$ and $\text{S33}_9(\text{V126-}b\text{-A69-g-N48}_{4,5})_9$]. This probably implies that the grafting chains inhibit the electrostatic interactions among the oppositely charged moieties located at the different segments, thus preventing precipitation and therefore allowing network formation. As the grafting density further increases [$\text{S33}_9(\text{V126-}b\text{-A69-g-N48}_{11})_9$ case], syneresis or even precipitation for $\text{S34}_{22}(\text{V136-}b\text{-A119-g-N48}_4)_{22}$ occurs, likely because the overall hydrophobicity of the star-graft cannot counterbalance the electrostatic repulsive interactions that preserve solubility in the macromolecules of lower grafting density and arm number.

4. Conclusions

In this work, novel multi-responsive quarterpolymers were designed exhibiting star-graft macromolecular architecture. The synthesis of these complex segmented macromolecules was accomplished by easy grafting of relatively short PNIPAM chains ($\text{DP}_n = 48$) through the carbodiimide approach onto the outer PAA block-arms of $\text{PS}_n(\text{P2VP-}b\text{-PAA})_n$ heteroarm star block terpolymers prepared by a multistep anionic polymerization method. To the best of our knowledge the resulting $\text{PS}_n(\text{P2VP-}b\text{-PAA-g-PNIPAM})_n$ heteroarm star graft quarterpolymer macromolecular topology appears for the first time.

Thanks to the nature of the various segments, P2VP/PAA pH-responsive weak polyelectrolytes and thermo-responsive PNIPAM, these star-graft quarterpolymers exhibited complex solution behavior in aqueous media. Their intermolecular association, induced by heating, is due to the well known coil-globule transition of the PNIPAM grafting chains occurring upon increasing their temperatures above their LCST. However since the PNIPAM chains have been grafted to a pH responsive star terpolymer bearing polyelectrolyte segments, this thermo-responsiveness was affected by various factors concerning either the solution conditions of pH and ionic strength or the polymer architecture, namely number of arms and PNIPAM grafting density.

The presence of PNIPAM grafts on the $PS_n(P2VP-b-PAA)_n$ stars not only endows these macromolecules with thermoresponsiveness but also with enhanced aqueous solution stability, preventing precipitation at the intermediate pH window (iep region), contrary to the behavior exhibited by their precursor. More interestingly, precipitation did not occur at iep even at elevated temperatures (above the LCST of PNIPAM), showing that the PNIPAM grafts likely hinder the electrostatic interactions among the oppositely charged segments ($2VPH^+$ vs. AA^-), located along the arms of the star.

Upon heating the aqueous star-graft solutions, an intermolecular association was observed above a critical temperature, defined as T_{ass} . This effect is due to the hydrophobic attractions of the PNIPAM sticking grafts above their LCST. T_{ass} is affected by a variety of factors namely pH and ionic strength, as well as the macromolecular characteristics such as the number of arms and the PNIPAM grafting density. Surprisingly, very weak intermolecular association was observed near the physiological pH for the low grafting density stars. In this case, the thermoresponsiveness comes out as an intramolecular effect.

At elevated concentrations and high temperatures, rich phase behavior was revealed by simple optical observations. More importantly, a gel phase was observed depending strongly on the solution pH and the grafting density along with the number of arms of the star-grafts. The gelation phenomenon is attributed to the formation of a transient 3D network arising from the extensive interstar hydrophobic association which however, is influenced by the pH-controlled electrostatic interactions along the arms. A sol to gel transition occurred upon cooling the gel phase, taking place at high temperature and low pH, proving the reversibility of the gelation phenomenon. This transition, as determined by oscillatory shear rheological experiments, was not affected noticeably by the grafting density. However, the latter factor affects remarkably the elastic modulus of the hydrogel; that is, the higher the PNIPAM grafting density the higher the elastic modulus. For instance, a strong physical gel, exhibiting elastic modulus of the order of 10^3 Pa s, was formed at a polymer concentration as low as 3 wt% for the sample having the highest PNIPAM grafting density.

Overall, these novel heteroarm star-graft quarterpolymers exhibit rich thermoresponsive behavior which can be tuned by

the pH and the ionic strength of the aqueous media and the tunable macromolecular characteristics. Their aqueous formulations, either in low or high polymer concentration, could find potential applications as “smart” multi-compartmentalized nanocarriers and/or hydrogels, which is the objective of further investigation.

Acknowledgements

M.M. Soledad Lencina would like to thank the State Scholarships Foundation (I.K.Y.) of Greece for the POSTDOCTORAL grant, supporting her 6-month stay in the Department of Chemical Engineering at the University of Patras. The authors thank Dr Maria Kollia from the Lab of Electron Microscopy and Microanalysis at the University of Patras for the TEM images.

Notes and references

- 1 K. Khanna, S. Varshney and A. Kakkar, *Polym. Chem.*, 2010, **1**, 1171.
- 2 Z. Iatridi and C. Tsitsilianis, *Polymers*, 2011, **3**, 1911.
- 3 H. Gao, *Macromol. Rapid Commun.*, 2012, **33**, 722.
- 4 X. Li, Y. Qjan, T. Liu, X. Hu, G. Zhang, Y. You and S. Liu, *Biomaterials*, 2011, **32**, 6595.
- 5 W. Cao, J. Zhou, A. Mann, Y. Wang and L. Zhu, *Biomacromolecules*, 2011, **12**, 2697.
- 6 K. Knop, D. Pretzel, A. Urbanek, T. Rudolph, D. H. Scharf, A. Schallon, M. Wagner, S. Schubert, M. Kiehntopf, A. A. Brakhage, F. H. Schacher and U. S. Schubert, *Biomacromolecules*, 2013, **14**, 2536.
- 7 Y.-Q. Yang, B. Zhao, Z.-D. Li, W.-J. Lin, C.-Y. Zhang, X.-D. Guo, J.-F. Wang and L.-J. Zhang, *Acta Biomater.*, 2013, **9**, 7679.
- 8 T. Terashima, M. Kamigaito, K.-Y. Baek, T. Ando and M. Sawamoto, *J. Am. Chem. Soc.*, 2003, **125**, 5288.
- 9 B. Helms, S. J. Guillaudeau, Y. Xie, M. McMurdo, C. J. Hawker and J. M. J. Frechet, *Angew. Chem., Int. Ed.*, 2005, **44**, 6384.
- 10 W. R. Dichtel, K.-Y. Baek, J. M. J. Frechet, I. B. Rietveld and S. A. Vinogradov, *J. Polym. Sci., Part A: Polym. Chem.*, 2006, **44**, 4939.
- 11 M. A. R. Meier, M. Filali, J.-F. Gohy and U. S. Schubert, *J. Mater. Chem.*, 2006, **16**, 3001.
- 12 Z. Iatridi and C. Tsitsilianis, *Soft Matter*, 2013, **9**, 185.
- 13 J. H. Youk, M.-K. Park, J. Locklin, R. Advincula, J. Yang and J. Mays, *Langmuir*, 2002, **18**, 2455.
- 14 I. Zhang, H. Niu, Y. Chen, H. Liu and M. Gao, *J. Colloid Interface Sci.*, 2006, **298**, 177.
- 15 C.-A. Fustin, C. Collard, M. Filali, P. Guillet, A.-S. Duwez, M. A. R. Meier, U. S. Schubert and J.-F. Gohy, *Langmuir*, 2006, **22**, 6690.
- 16 Z. Shen, H. Duan and H. Frey, *Adv. Mater.*, 2007, **19**, 349.
- 17 Q. Qiu, G. Liu and Z. An, *Chem. Commun.*, 2011, **47**, 12685.

- 18 W. Li, Y. Yu, M. Lamson, M. S. Silverstein, R. D. Tilton and K. Matyjaszewski, *Macromolecules*, 2012, **45**, 9419.
- 19 X. Shi, M. Miao and Z. An, *Polym. Chem.*, 2013, **4**, 1950.
- 20 J. Deng, N. Li, K. Mai, C. Yang, L. Yan and L.-M. Zhang, *J. Mater. Chem.*, 2011, **21**, 5273.
- 21 K. S. Pafiti, N. P. Mastroyiannopoulos, I. A. Phylactou and C. S. Patrickios, *Biomacromolecules*, 2011, **12**, 1468.
- 22 (a) Z. Li, E. Kesselman, Y. Talmon, M. A. Hillmyer and T. P. Lodge, *Science*, 2004, **98**(306), 98; (b) Z. Li, M. A. Hillmyer and T. P. Lodge, *Langmuir*, 2006, **22**, 9409; (c) N. Saito, C. Liu, T. P. Lodge and M. A. Hillmyer, *Macromolecules*, 2008, **41**, 8815; (d) N. Saito, C. Liu, T. P. Lodge and M. A. Hillmyer, *ACS Nano*, 2010, **4**, 1907.
- 23 A. Walther and A. H. E. Muller, *Chem. Commun.*, 2009, 1127.
- 24 J. Li, W.-D. He, N. He, S.-C. Han, X.-L. Sun, L.-Y. Li and B.-Y. Zhang, *J. Polym. Sci., Part A: Polym. Chem.*, 2009, **47**, 1450.
- 25 K. Van Butsele, J. F. Gohy, R. Jerome and C. Jerome, *Langmuir*, 2009, **25**, 107.
- 26 (a) H. Liu, C. Li, H. Liu and S. Liu, *Langmuir*, 2009, **25**, 4724; (b) Y. Zhang, H. Liu, J. Hu, C. Li and S. Liu, *Macromol. Rapid Commun.*, 2009, **30**, 941; (c) Y. Zhang, H. Liu, H. Dong, C. Li and S. Liu, *J. Polym. Sci., Part A: Polym. Chem.*, 2009, **47**, 1636.
- 27 Y.-Y. Yuan and J. Wang, *Colloids Surf., B: Biointerfaces*, 2011, **85**, 81.
- 28 (a) N. Stavrouli, A. I. Triftaridou, C. S. Patrickios and C. Tsitsilianis, *Macromol. Rapid Commun.*, 2007, **28**, 560; (b) A. I. Triftaridou, M. Vamvakaki, C. S. Patrickios, N. Stavrouli and C. Tsitsilianis, *Macromolecules*, 2005, **38**, 1021.
- 29 W. Zhu, A. Nese and K. Matyjaszewski, *J. Polym. Sci., Part A: Polym. Chem.*, 2011, **49**, 1942.
- 30 C. Tsitsilianis, G. Gotzamanis and Z. Iatridi, *Eur. Polym. J.*, 2011, **47**, 497.
- 31 W. Zhang, W. Zhang, N. Zhou, J. Zhu, Z. Cheng and X. Zhu, *J. Polym. Sci., Part A: Polym. Chem.*, 2009, **47**, 6304.
- 32 (a) N. Stavrouli, A. Kyriazis and C. Tsitsilianis, *Macromol. Chem. Phys.*, 2008, **209**, 2241; (b) I. Choi, R. Gunawidjaja, R. Suntivich, C. Tsitsilianis and V. V. Tsukruk, *Macromolecules*, 2010, **43**, 6818; (c) Z. Iatridi and C. Tsitsilianis, *Chem. Commun.*, 2011, **47**, 5560; (d) Z. Iatridi, Y. Roiter, N. Stavrouli, S. Minko and C. Tsitsilianis, *Polym. Chem.*, 2011, **2**, 2037.
- 33 R. C. Hayward and D. J. Pochan, *Macromolecules*, 2010, **43**, 3577.
- 34 K. Ishizu and S. Uchida, *Prog. Polym. Sci.*, 1999, **24**, 1439.
- 35 N. Hadjichristidis, *J. Polym. Sci., Part A: Polym. Chem.*, 1999, **37**, 857.
- 36 R. P. Quirk, T. Yoo, Y. Lee, J. Kim and B. Lee, *Adv. Polym. Sci.*, 2000, **153**, 67.
- 37 N. Hadjichristidis, M. Pitsikalis, S. Pispas and H. Iatrou, *Chem. Rev.*, 2001, **101**, 3747.
- 38 A. Hirao, M. Hayashi, S. Loykulnant, K. Sugiyama, S. W. Ryu, N. Haraguchi, A. Matsuo and T. Higashihara, *Prog. Polym. Sci.*, 2005, **30**, 111.
- 39 N. Hadjichristidis, M. Pitsikalis and H. Iatrou, *Adv. Polym. Sci.*, 2005, **189**, 1.
- 40 H. Gao and K. Matyjaszewski, *Prog. Polym. Sci.*, 2009, **34**, 317.
- 41 G. Lapienis, *Prog. Polym. Sci.*, 2009, **34**, 852.
- 42 G. Linardatos, G. Tsoukleri, J. Parthenios, C. Galiotis, O. Monticelli, S. Russo and C. Tsitsilianis, *Macromol. Rapid Commun.*, 2011, **32**, 371.
- 43 M. Zhang, H. Liu, W. Shao, C. Ye and Y. Zhao, *Macromolecules*, 2012, **45**, 9312.
- 44 Y. Deng, S. Zhang, G. Lu and X. Huang, *Polym. Chem.*, 2013, **4**, 1289.
- 45 J. Zhao, D. Pahovnik, Y. Gnanou and N. Hadjichristidis, *J. Polym. Sci., Part A: Polym. Chem.*, 2015, **53**, 304.
- 46 (a) D. Voulgaris and C. Tsitsilianis, *Macromol. Chem. Phys.*, 2001, **202**, 3284; (b) A. Kiriy, G. Gorodyska, S. Minko, M. Stamm and C. Tsitsilianis, *Macromolecules*, 2003, **36**, 8704; (c) G. Gorodyska, A. Kiriy, S. Minko, C. Tsitsilianis and M. Stamm, *Nano Lett.*, 2003, **3**, 365; (d) M. Stepanek, P. Matejcek, J. Humpolickova, J. Havrankova, K. Podhajecka, M. Spirkova, Z. Tuzar, C. Tsitsilianis and K. Prochazka, *Polymer*, 2005, **46**, 10493; (e) A. Kyriazis, T. Aubry, W. Burchand and C. Tsitsilianis, *Polymer*, 2009, **50**, 3204.
- 47 J. Teng and E. R. Zubarev, *J. Am. Chem. Soc.*, 2003, **125**, 11840.
- 48 Y. Cai and S. P. Armes, *Macromolecules*, 2005, **38**, 271.
- 49 S. Strandman, A. Zarembo, A. A. Darinskii, B. Loflund, S. J. Butcher and H. Tenhu, *Polymer*, 2007, **48**, 7008.
- 50 E. He, P. Ravi and K. C. Tam, *Langmuir*, 2007, **23**, 2382.
- 51 J. Rao, Y. Zhang, J. Zhang and S. Liu, *Biomacromolecules*, 2008, **9**, 2586.
- 52 K. Tao, Y. Wang, W. Wang, D. Lu, Y. Wang and R. Bai, *Macromol. Chem. Phys.*, 2009, **210**, 478.
- 53 C. Liu, M. A. Hillmyer and T. P. Lodge, *Langmuir*, 2009, **25**, 13718.
- 54 X. Zhang, Y. Xiao and M. Lang, *J. Macromol. Sci., Pure Appl. Chem.*, 2014, **51**, 63.
- 55 Z. Wu, H. Liang and J. Lu, *Macromolecules*, 2010, **43**, 5699.
- 56 C. Li, Z. Ge, H. Liu and S. Liu, *J. Polym. Sci., Part A: Polym. Chem.*, 2009, **47**, 4001.
- 57 J. Li, W.-D. He, S.-C. Han, X.-L. Sun, L.-Y. Li and B.-Y. Zhang, *J. Polym. Sci., Part A: Polym. Chem.*, 2009, **47**, 786.
- 58 (a) Y. Cai, C. Burguiere and S. P. Armes, *Chem. Commun.*, 2004, 802; (b) Y. Cai, Y. Tang and S. P. Armes, *Macromolecules*, 2004, **37**, 9728; (c) Z. Ge, Y. Cai, J. Yin, Z. Zhu, J. Rao and S. Liu, *Langmuir*, 2007, **23**, 1114.
- 59 Z. Ge, J. Xu, J. Hu, Y. Zhang and S. Liu, *Soft Matter*, 2009, **5**, 3932.
- 60 (a) F. A. Plamper, J. R. McKee, A. Laukkanen, A. Nykänen, A. Walther, J. Ruokolainen, V. Aseyev and H. Tenhu, *Soft Matter*, 2009, **5**, 1812; (b) F. A. Plamper, A. Schmalz,

- M. Ballauff and A. H. E. Muller, *J. Am. Chem. Soc.*, 2007, **129**, 14538.
- 61 X. Huang, Y. Xiao and M. Lang, *Macromol. Res.*, 2011, **19**, 113.
- 62 M. R. Hammond, C. Li, C. Tsitsilianis and R. Mezzenga, *Soft Matter*, 2009, **5**, 2371.
- 63 C. Tsitsilianis, D. Voulgaris, M. Stepanek, K. Prodhajicka, K. Prochazka, Z. Tuzar and W. Brown, *Langmuir*, 2000, **16**, 6868.
- 64 A. Durand and D. Hourdet, *Polymer*, 1999, **40**, 4941.
- 65 G. Staikos, G. Bokias and K. Karayanni, *Polym. Int.*, 1996, **41**, 345.